RAPID COMMUNICATIONS

PHYSICAL REVIEW B VOLUME 46, NUMBER 19 15 NOVEMBER 1992-I

Quantum conductance of point contacts in Si inversion layers

S. L. Wang, P. C. van Son,* B. J. van Wees, and T. M. Klapwijk
Department of Applied Physics and Materials Science Centre, University of Groningen, Nijenborgh 4, 9747 AG Groningen, The Netherlands
(Received 30 July 1992)

We have performed electron-transport studies on high-mobility Si inversion layers in which a narrow and short constriction is defined electrostatically. When the width of the constriction is varied, steplike structures in the conductance are observed with a spacing of approximately $4e^2/h$ in zero magnetic field and at a temperature of 1.2 K. In the presence of a magnetic field these features develop into quantum Hall plateaus and the fourfold degeneracy is lifted. We argue that this behavior arises from the depopulation of successive one-dimensional subbands in the constriction.

Si inversion layers are excellent systems to study many aspects of the two-dimensional (2D) electron transport. During the past decade a number of papers have been published about the conductance of metal-oxide-semiconductor field-effect transistors (MOSFET's) in which the electronic states are confined in a second direction, providing a system to study transport in one dimension. Such a confinement has been achieved by using either a physical boundary[1] or an electrostatic potential.[2,3] For single-narrow-wire MOSFET's, in the diffusive transport regime, random but reproducible conductance fluctuations are observed which wash out the expected structure due to 1D subbands.[1] This behavior has been attributed to random variations in the potential well at the boundary. Later on, devices containing a few hundred parallel wires have been studied in an attempt to average out these fluctuations. Indeed a weak oscillation of the transconductance with gate voltage has been reported.[2] Recently so-called dual-gate geometries have been studied.[3] One gate defines the 2D electron gas (2DEG) while the second one changes the width of the channel continuously by using the field effect. In addition, short-length contacts can be made to get into the ballistic regime avoiding the strong scattering in long 1D wires. Until now 1D quantization as observed in point contacts in $GaAs/Al_xGa_{1-x}As$ heterostructures[4] has not been observed in Si MOSFET's. A crucial problem is that those devices have low mobilities.[1-3] It results in a relatively short elastic scattering length (l_e) and only transport in the diffusive regime can be studied.

In this paper, we present experimental results of the resistance of point contacts in Si inversion layers in the ballistic regime. Using high-mobility Si MOSFET's, the dimensionality of the electrons in the Si inversion layer is changed from 2D to quasi-1D by using an electrode configuration. A narrow and short constriction is defined electrostatically using a single gate. An essential advantage is that the channel wall defined by the confining potential is much smoother than the one defined by a physical boundary. Second, the high mobility results in an elastic scattering length which is of the order of the length of the constriction. When the width of the constriction is varied, steplike features are found in the conductance with a spacing of approximately $4e^2/h$.

The measurements are based on Si MOSFET's which have peak mobilities of 2.2 $m^2 V^{-1} s^{-1}$ at a carrier concentration of 5.6×10^{15} m^{-2} measured at a temperature of 1.2 K. A 100-nm-thick gate oxide is thermally grown on p-type Si (100) wafers. Tungsten is used for the gate metallization to allow for dry etching. We start out with a standard Hall bar geometry. To establish the confinement we use submicrometer gaps in the gate metallization [see Fig. 1(a)]. The submicrometer gaps are defined by electron beam lithography and by reactive ion etching. In the region where the gaps cross, the width and length of the opening are both approximately 200 nm (from scanning electron microscopy). The gaps are sufficiently narrow compared to the oxide thickness to prevent the formation of a barrier between different sections of the 2DEG.[5] After processing of the submicrometer gaps and an anneal step the peak mobility of the sample maintains its value, resulting in a maximum elastic scattering length (l_e) of 190 nm. The conduction-band bending associated with the interrupted-gate geometry is shown schematically in Fig. 1(b). A positive voltage V_g on the longitudinal pair of gate electrodes along the Hall bar determines the Fermi energy E_F in the wide 2DEG. The confining potential is established by applying a voltage V_{pg}, which is lower than the threshold voltage V_{th}, on the transverse pair of gate electrodes. A saddle-shape potential is formed in the inversion layer and the electrons are laterally confined in the crossing region underneath the gaps. The width of the confinement (W_{eff}) and the barrier height (eV_0) relative to the bottom of the conduction band in the wide 2DEG are determined by the combination of V_g and V_{pg}. In the following the transverse pair of gate electrodes will be indicated as the pinch gate.

Four terminal resistances across the constriction as a function of V_{pg} are measured at fixed V_g in zero magnetic field and at 1.2 K. A small ac current is sent from contacts i to j and the voltage difference between contacts k and l is measured with a lock-in amplifier. The resulting resistance is denoted by $R_{ij,kl}$. The threshold voltage of the sample is 1.2 V which is determined from

 ©1992 The American Physical Society

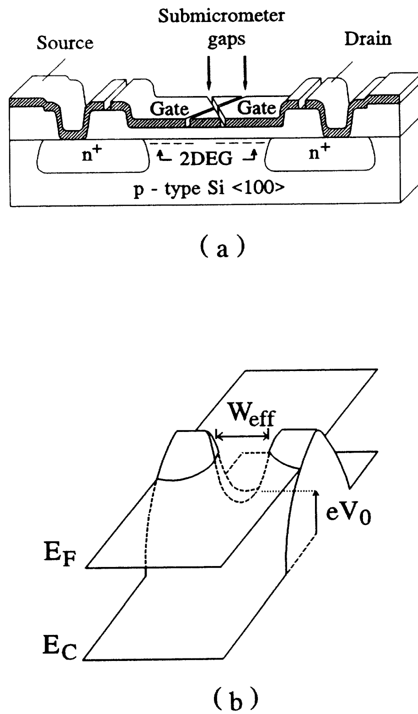

FIG. 1. (a) Schematic cross section of the device used in these experiments. The device has an overall length of 800 μm, and a width of 50 μm. The width of the submicrometer gaps is about 0.1 μm. (b) Saddle-shape potential landscape at the Si/SiO_2 interface along the Hall bar when the point contacts are formed. The Fermi energy E_F in the wide 2DEG is determined by the gate voltage V_g. The width of the constriction W_{eff} and the barrier height (eV_0) are determined by the combination of V_g and the pinch-gate voltage V_{pg}.

Shubnikov–de Haas (SdH) oscillations when V_g and V_{pg} have an identical positive bias. The 2DEG underneath the pinch-gate electrode is depleted completely when V_{pg} is less than 1.2 V, where the point contact is formed, shown in Fig. 2 as a drastic drop in conductance. The width of the constriction (W_{eff}) is gradually reduced by a further decrease in V_{pg} until the conductance is fully pinched off.

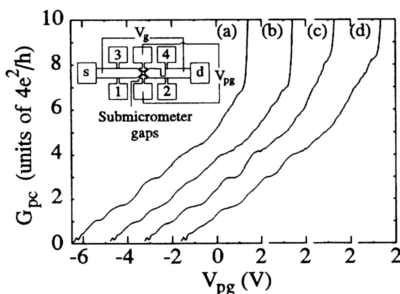

FIG. 2. Point-contact conductance as a function of V_{pg} in zero magnetic field and at 1.2 K for different V_g. The point contact is formed at $V_{\text{pg}} \approx 1.2$ V. Curves (*b*)–(*d*) have been offset horizontally for clarity. The inset shows a top view of the device (Hall-bar geometry with a narrow strip 30 μm long, and 2 μm wide) (not to scale).

The measured resistances are $G_{\text{exp}}^{-1}(=R_{sd,14})=G_{\text{pc}}^{-1}+G_s^{-1}$, where G_{pc}^{-1} is the resistance of the point contact and G_s^{-1} is the constant series resistance adjacent to the point contacts. Based on the geometry of the gate metallization and the measured resistivity of the 2DEG we can determine this series resistance G_s^{-1}. The number of $R_\square$'s for our samples is (26.2±0.5); the uncertainty is due to details in the shape of the constriction. Following the multichannel Landauer formula,[6] the point-contact conductance is

$$G_{\text{pc}}=g_s g_v \frac{e^2}{h}\sum_{n=1}^{N} T_n(E_F) , \quad (1)$$

where T_n is the transmission probability at the Fermi energy and the factors g_s and g_v account for the spin degeneracy and valley degeneracy, respectively. If no backscattering takes place, the sum of $T_n(E_F)$ is equal to N. A step-wise increase in the conductance of an ideal 1D conductor is expected when the number of occupied subbands is increased. As demonstrated in Fig. 2, the point-contact conductance, as calculated from the G_{exp}^{-1} by subtracting the G_s^{-1}, shows steplike features with approximately the expected spacing of $4e^2/h$ [for silicon (100) $g_s=g_v=2$]. The gate voltages V_g are varied from 17.4 to 20.4 V in steps of 1 V. The subtracted values for curves (*a*)–(*d*) are 6420, 6450, 6610, and 6760 Ω, respectively.

Assuming a parabolic confining potential $V(x)=V_0+m^*\omega_0^2x^2/2e$, W_{eff} at the Fermi level E_F can be expressed as $W_{\text{eff}}=2[2(E_F-eV_0)/m^*]^{1/2}/\omega_0$, where $m^*(=0.19m_0)$ is the effective mass of the electrons. When $V_g=19.4$ V [Fig. 2(c)], the Fermi energy is equal to 25.7 meV ($dE_F/dV_g=1.41$ meV/V for the sample reported here). The barrier height eV_0 is taken from the high-field magnetoconductance for V_{pg} just below the formation of the point contact. At $B=12$ T, the point-contact conductance in units $(4e^2/h)$ is $(E_F-eV_0)/\hbar\omega_c \approx 1.16$, where $\hbar\omega_c$ is the Landau-level separation leading to $eV_0=17.2$ meV. From Fig. 2(c), the conductance value when the point contact is just formed corresponds to eight occupied subbands. Therefore the subband spacing $\hbar\omega_0$ is equal to 1.1 meV, which means that W_{eff} at the Fermi level is equal to 170 nm. For the other curves in Fig. 2 similar values for $\hbar\omega_0$ and W_{eff} are obtained. As expected, W_{eff} is smaller than the lithographic width because of the fringing fields contributing to the confining potential. In this analysis we assume the transmission coefficient for each subband is equal to one and fourfold degeneracy. A much wider constriction would be required if either the transmission would be substantially less than unity or the subbands are not fourfold degenerate.

We have also investigated the behavior of these point contacts in magnetic fields applied perpendicular to the 2DEG. The magnetic field creates hybrid magnetoelectric subbands and changes the dispersion relation of the electron waves. For a parabolic model, the dispersion of the 1D subbands can be written as $E_n(\kappa)=(n-\frac{1}{2})\hbar\omega+(1/2m^*)(\omega_0^2/\omega^2)\hbar^2\kappa^2$ with $\omega^2=\omega_0^2+\omega_c^2$, where $\omega_c=eB/m^*$ is the cyclotron frequency.[7] In a magnetic

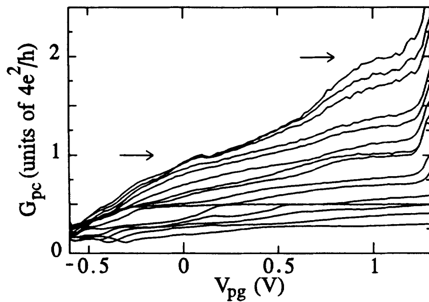

FIG. 3. Point-contact conductance as a function of V_{pg} at various magnetic fields, and at a temperature of 75 mK (from top to bottom $B=0$, 1, 1.5, 2, 2.3, 2.7, 3.3, 3.5, 4.1, 4.6, 5.7, 6.5, 7.6, 9.2, and 11.5 T, respectively).

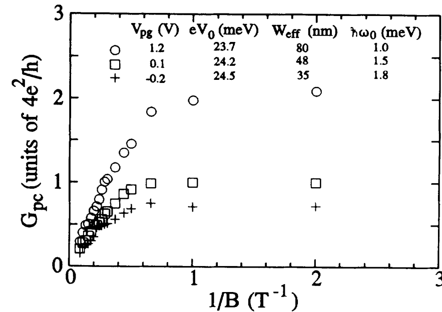

FIG. 4. Point-contact conductance of Fig. 3 as a function of reciprocal magnetic field for several fixed pinch-gate voltages.

field of 1 T, the conductance at V_{pg} where the point contact is formed has decreased to a value corresponding to seven occupied subbands. Using the same analysis as before we find a subband spacing $\hbar\omega=1.2$ meV and therefore $\hbar\omega_0=1.0$ meV. This is consistent with the previous estimate from the conductance in zero magnetic field.

Continuing our analysis in terms of quantum ballistic transport [Eq. (1)] we expect plateaus in the conductance at multiples of $4e^2/h$. As is evident from Fig. 2 steplike features in the point-contact conductance are clearly visible. Some plateaus are at multiples of $4e^2/h$, some are at lower values, and some are absent. These steplike features are observed in 28 samples out of four different batches. Only in two of them do the steps show up as clearly as in Fig. 2. All samples for similar V_g have conductances consistent with the transmission of eight subbands at the pinch-gate voltage where the point contact is formed. This pattern does not change significantly upon cooling to 100 mK. We attribute the variation in visibility of the plateaus to impurities located in or close to the point contacts. Similar behavior has been found in $GaAs/Al_xGa_{1-x}As$ heterostructures.[8] Calculations demonstrate that the visibility of steps in the conductance depends strongly on the exact configuration of the impurity.[9] The presence of an isolated conductance peak near pinch-off (Fig. 2) also points to the relevance of impurities in our point contacts. In addition, we point out that the quality of the steplike features is best when V_g is between 17 and 20 V. Interestingly, this corresponds to an electron density in the point contact comparable to that when the mobility has a maximum.

Figure 3 shows the conductance G_{pc} of an apparently narrower point contact as a function of V_{pg} in a magnetic field ranging from 0 to 11.5 T oriented perpendicular to the 2DEG and at a temperature down to 75 mK. For given identical V_g and V_{pg} a magnetic field is selected where ρ_{xx} is minimum. The value of ρ_{xx} timing the number of squares is subtracted from G_{exp}^{-1} to obtain G_{pc}^{-1}. In the quantum Hall regime where the minimum value of ρ_{xx} is zero this procedure leads to $G_{pc}^{-1}=G_{exp}^{-1}$. Although V_g is again 19.4 V, the corresponding number of occupied subbands (when $V_{pg}=1.2$ V) is slightly more than two. In zero magnetic field, the point-contact conductance shows structures at multiples of $4e^2/h$ indicated by arrows (see Fig. 3). When the magnetic field is increased, the conductance decreases gradually and does not show fluctuations (except near pinch-off). The plateaulike features at $4e^2/h$ develop into entirely flat quantized Hall plateaus. In high fields the spin degeneracy and valley degeneracy are lifted and additional plateaus appear at multiples of e^2/h. The conductance as a function of reciprocal magnetic field is shown in Fig. 4. It reveals the characteristic signature of magnetic depopulation of 1D subbands.[7] Clear deviation from the 2D behavior appears at a value of $B\approx2$ T and the curve saturates at high values of $1/B$. The derived values for eV_0, $\hbar\omega_0$, and W_{eff} are given in Fig. 4. These numbers are consistent with the overall picture of $4e^2/h$ quantization in a relatively narrow point contact.

In summary, we report measurements of the conductance of point contacts in Si inversion layers in the ballistic regime. Steplike features in the conductance with a spacing of $4e^2/h$ are observed indicative of quantum-ballistic transport through fourfold degenerate 1D subbands. The smooth transition from zero-field quantized conduction to the quantum Hall effect provides a direct demonstration of the magnetic depopulation of 1D subbands.

We thank S. Bakker for the skillful preparation of high-quality MOSFET's, O. J. Homan for assistance in the measurements, and R. G. Wheeler, A. B. Fowler, L. W. Molenkamp, B. W. Alphenaar, and J. R. Gao for valuable discussions. We thank J. H. Davies and co-workers for communicating their results (Ref. 1) prior to publication. This work was supported by Stichting voor Fundamenteel Onderzoek der Materie (FOM). The research of P.C.v.S. was supported by the Royal Netherlands Academy of Arts and Sciences.

*Present address: Department of Applied Physics, Delft University of Technology, Lorentzweg 1, 2628 CJ Delft, The Netherlands.

[1]Si MOSFET's with a single channel: W. J. Skocpol, L. D. Jackel, R. E. Howard, H. G. Craighead, L. A. Fetter, P. M. Mankiewich, P. Grabbe, and D. M. Tennant, Surf. Sci. **142**, 14 (1984). For recent experiments see K. Takeuchi and R. Newbury, Phys. Rev. B **43**, 7324 (1991), and Y. S. Tang, G. Jin, J. H. Davies, J. G. Williamson, and C. D. W. Wilkinson, *ibid.* **45**, 13 799 (1992).

[2]Si MOSFET's with multiple channels: A. C. Warren, D. A. Antoniadis, and H. I. Smith, Phys. Rev. Lett. **56**, 1858 (1986); J. R. Gao, C. de Graaf, J. Caro, S. Radelaar, M. Offenberg, V. Lauer, J. Singleton, T. J. B. M. Janssen, and J. A. A. J. Perenboom, Phys. Rev. B **41**, 12 315 (1990).

[3]Si MOSFET's with dual-gate geometries: C. de Graaf, J. Caro, S. Radelaar, V. Lauer, and K. Heyers, Phys. Rev. B **44**, 9072 (1991); H. Matsuoka, T. Ichiguchi, T. Yoshimura, and E. Takeda, IEEE Electron Dev. Lett. **13**, 20 (1992).

[4]B. J. van Wees, H. van Houten, C. W. Beenakker, J. G. Williamson, L. P. Kouwenhoven, D. van der Marel, and C. T. Foxon, Phys. Rev. Lett. **60**, 848 (1988); D. A. Wharam, T. J. Thornton, R. Newbury, M. Pepper, H. Ahmed, J. E. F. Frost, D. G. Hasko, D. C. Peacock, D. A. Ritchie, and G. A. C. Jones, J. Phys. C **21**, L209 (1988).

[5]S. L. Wang, P. C. van Son, S. Bakker, and T. M. Klapwijk, J. Phys. C **3**, L4297 (1991).

[6]R. Landauer, IBM J. Res. Dev. **1**, 223 (1957); Phys. Lett. **85A**, 91 (1981); J. Phys. C **1**, 8099 (1989).

[7]K.-F. Berggren, T. J. Thornton, D. J. Newson, and M. Pepper, Phys. Rev. Lett. **57**, 1769 (1986).

[8]P. L. McEuen, B. W. Alphenaar, and R. G. Wheeler, Surf. Sci. **229**, 312 (1990).

[9]D. van der Marel and E. G. Haanappel, Phys. Rev. B **39**, 7811 (1989); J. A. Nixon, J. H. Davies, and H. U. Baranger, Superlatt. Microstruct. **9**, 187 (1991).